The N-terminal region of the starch-branching enzyme from *Phaseolus vulgaris* L. is essential for optimal catalysis and structural stability

Shigeki Hamada [a], Hiroyuki Ito [a,*], Hiroshi Ueno [a], Yasuhito Takeda [b], and Hirokazu Matsui [a]

[a] *Division of Applied Bioscience, Graduate School of Agriculture, Hokkaido University, Sapporo 060-8589, Japan*

[b] *Department of Biochemical Science and Technology, Kagoshima University, Kagoshima 890-0065, Japan*

*Corresponding author. Tel./fax: +81 11 706 2508

E-mail address: otih@chem.agr.hokudai.ac.jp (H. Ito)

Abbreviations: SBE, starch-branching enzyme; GBE, glycogen-branching enzyme; dp, degree of polymerization; HPAEC–PAD, high-performance anion exchange chromatography–pulsed amperometric detector; PvSBE, kidney bean (*Phaseolus vulgaris* L.) SBE; (1Na/2Nb)-II, N-terminal chimeric enzyme between PvSBE1 and PvSBE2; ΔN46-PvSBE2, N-terminal truncated form of PvSBE2; D15A-, D15E-, H24A-, R28A-, and R28K-PvSBE2, site-directed mutant forms of PvSBE2.

Abstract

Starch-branching enzymes (SBEs) play a pivotal role in determining the fine structure of starch by catalyzing the syntheses of α-1,6-branch points. They are the members of the α-amylase family and have four conserved regions in a central $(\beta/\alpha)_8$ barrel, including catalytic sites. Although the role of the catalytic barrel domain of an SBE is known, that of its N- and C-terminal regions remains unclear. We have previously shown that the C-terminal regions of the two SBE isozymes (designated as PvSBE1 and PvSBE2) from kidney bean (*Phaseolus vulgaris* L.) have different roles in branching enzyme activity. To understand the contribution of the N-terminal region to catalysis, six chimeric enzymes were constructed between PvSBE1 and PvSBE2. Only one enzyme (1Na/2Nb)-II, in which a portion of the N-terminal region of PvSBE2 was substituted by the corresponding region of PvSBE1, retained 6% of the PvSBE2 activity. The N-terminal truncated form (ΔN46-PvSBE2), lacking 46 N-terminal residues of PvSBE2, lost the enzyme activity and stability to proteolysis. To investigate the possible function of this region, three residues (Asp-15, His-24, and Arg-28) among these 46 residues were subjected to site-directed mutagenesis. The purified mutant enzymes showed nearly the same K_m values as PvSBE2 but had lower V_{max} values and heat stabilities than PvSBE2. These results suggest that the N-terminal region of the kidney bean SBE is essential for maximum enzyme activity and thermostability.

Keywords: kidney bean (*Phaseolus vulgaris* L.); chimeric enzyme; site-directed mutagenesis; starch-branching enzyme; kinetics

1. Introduction

Plant starch biosynthesis is mediated by at least four kinds of enzymes: ADP-glucose pyrophosphorylases, starch synthases, starch-branching enzymes (SBEs), and starch-debranching enzymes. The coordinated functions of these enzymes result in two types of α-glucan: amylose and amylopectin. Amylose is essentially a linear molecule composed of α-1,4-glucosidic linkages, and amylopectin has a much highly branched glucan chain with multiple branch points formed by α-1,6 linkages (Manners, 1989).

SBE (1,4-α-D-glucan: 1,4-α-D-glucan 6-α-D-(1,4-α-D-glucano) transferase, EC 2.4.1.18) catalyzes the cleavage of an α-1,4-glucosidic bond and the subsequent transfer of an α-1,4-oligosaccharide chain to form an α-1,6 branch point (Borovsky et al., 1976). SBE has an important role in determining the amylopectin structure of starch. Multiple forms of SBE have been identified in many plants, including cereal endosperms (Boyer and Preiss, 1978; Nakamura et al., 1992; Mizuno et al., 1993; Nagamine et al., 1997), pea embryo (Smith, 1988), and potato tuber (Koßmann et al., 1991; Poulsen and Kreiberg, 1993). A sequence comparison of SBEs from different plants indicates that they can be classified into two families, A and B. Family A SBEs show a lower affinity for amylose than family B SBEs and preferentially catalyze the transfer of chains shorter than those catalyzed by the latter (Takeda et al., 1993). Plant SBEs and bacterial glycogen-branching enzymes (GBEs) belong to the α-amylase family (Romeo et al., 1988; Baba et al., 1991; Takata et al., 1992; Kuriki and Imanaka,

1999). Based on the primary sequence alignments, secondary structure prediction, and three-dimensional structures of the α-amylase family members, SBEs are found to contain three domains: an amino-terminal (N) domain, a carboxyl-terminal (C) domain, and a central catalytic $(\beta/\alpha)_8$ barrel domain (Svensson, 1994; Abad et al., 2002). Because the central barrel regions of the SBEs of the families A and B share a significant homology with each other, it is assumed that their distinct enzymatic characteristics are largely attributable to the difference in their N- and C-domains. Several chimeric mutants of maize SBEs have been created and analyzed to understand the role of the three domains in branching enzyme activity. These studies indicated that an N-terminal region is important for specifying the chain length and is required for maximum enzyme activity (Kuriki et al., 1997; Hong et al., 2001), whereas a C-terminal region is involved in substrate specificity (Kuriki et al., 1997; Hong and Preiss, 2000). In kidney bean (*Phaseolus vulgaris* L.), two cDNA clones—pvsbe1 and pvsbe2—for SBE isozymes (designated PvSBE1 and PvSBE2, respectively) were isolated from developing seeds and expressed in *Escherichia coli* to investigate their enzymatic properties (Hamada et al., 2001). Our previous studies on chimeric and truncated mutants have shown that the C-terminal regions of the two PvSBEs have different roles in branching enzyme activity; the C-terminal region of PvSBE1 confers specificity to amylose, while that of PvSBE2 is responsible for specific catalysis of the transfer of short chains (Ito et al., 2004). A study on the three-dimensional structure of *E. coli* N113BE, which is an N-terminal truncated GBE, revealed that its N-domain contains a seven-stranded β-sandwich and that both N- and C-domains of this enzyme are

structurally similar to those of isoamylase and α-amylase (Abad et al., 2002). However, it is still difficult to predict the three-dimensional structures of plant SBEs, particularly that of their N-domains, based on the three-dimensional structures of *E. coli* N113BE; this is because of the low homology between their primary sequences and lack of the first 113 amino acids in N113BE.

In this study, to determine the role of the N-terminal region in SBE function, we constructed a series of chimeric enzymes containing swapped N-terminal regions of PvSBE1 and PvSBE2 from *Phaseolus vulgaris* L. Only one of the chimeric enzymes displayed significant branching enzyme activity and showed changes in the kinetic parameters. Moreover, the analysis of the N-terminal truncated and site-directed mutant forms indicated that the N-terminal region of an SBE is important for the maximum activity to amylose as a substrate and for the thermostability of the enzyme. Based on the results obtained in this study, we discuss a hypothetical model for the relationship between the structure and function of the N-domains in PvSBE isozymes.

2. Results and discussion

2.1. Enzymatic properties of (1Na/2Nb)-II chimeric enzyme

Plant SBEs are classified into two families, A and B, depending on the variation in the specific activity, specificity of the transferred chain length, and substrate preference. However, little is known about the structural features responsible for these characteristics. Our previous report on the C-terminal chimeric enzymes suggested that the C-terminal regions of the two PvSBE isozymes —PvSBE1 and PvSBE2— from *Phaseolus vulgaris* L. have different roles in branching enzyme activity (Ito et al., 2004).

To understand the function of the N-terminal region in specifying branching enzyme properties, expression vectors were constructed to generate six chimeric enzymes containing different segments of the N-terminal regions of PvSBE1 and PvSBE2 (Fig. 1). The measurement of branching enzyme activity by assay I in the cell extracts harboring recombinant plasmids showed that only one chimeric recombinant protein ((1Na/2Nb)-II) had enzyme activity (30 mU/mg of protein; Fig. 1), although recombinant proteins were found in the soluble extracts from cells expressing the six expression plasmids (data not shown). The other five recombinant proteins had negligible or no activity over endogenous background levels (less than 10 mU/mg of protein).

To obtain further information on the kinetic parameters and reaction products of

(1Na/2Nb)-II, the recombinant protein was purified to homogeneity as a single polypeptide band on SDS-PAGE gel (data not shown). When the purified (1Na/2Nb)-II was analyzed by assay I using amylose as a substrate, its specific activity was found to be 13 U/mg in the presence of 0.1 M citrate or 6.1 U/mg in the absence of citrate (Table 1). Citrate has been often used for the activation and stabilization of plant SBEs and bacterial GBEs. In the presence of 0.3 M citrate, the activity of (1Na/2Nb)-II increased 5.3-fold, and the degree of activation of (1Na/2Nb)-II was approximately 1.7-fold higher than that of PvSBE2. Unlike PvSBE2, the N-terminal chimeric enzyme was activated with a higher concentration of citrate, and its activity in the presence of 0.5 M citrate was approximately 7.5-fold higher than that in its absence (Fig. 2A). Although the mechanism for citrate activation is still unclear, our data show that the effect of citrate on SBE activity is possibly attributed to an interaction between citrate and the enzyme rather than an alteration of the physical nature of the substrate (Edwards et al., 1999; Hamada et al., 2001; Nozaki et al., 2001; Ito et al., 2004).

The kinetic parameters of the purified (1Na/2Nb)-II were analyzed using amylose as a substrate and compared with those obtained for PvSBE1 and PvSBE2 (Table 1). The Lineweaver–Burk plots for the reaction catalyzed by (1Na/2Nb)-II yielded K_m and V_{max} values of 0.63 mg/ml and 10 U/mg, respectively. The large decrease in the specific activity of (1Na/2Nb)-II was predominantly attributed to the reduced V_{max} value. These results suggest that the N-domain of PvSBEs closely interacts with the central $(\beta/\alpha)_8$-barrel domain. The chimeric enzymes in which the Nb segment was substituted showed no enzyme activity. One possible explanation for the unsuccessful

substitution is that the Nb segment is a part of the catalytic domain. Because the segment contains the first sheet, first helix, and second sheet of the $(\beta/\alpha)_8$ barrel, the displacement had a critical impact on the conformation of the catalytic domain.

A previous analysis of chain-length distribution performed using a high-performance anion exchange chromatography–pulsed amperometric detector (HPAEC–PAD) had revealed that the transferred products generated in vitro by PvSBE2 were predominantly short chains (degree of polymerization (dp) 6–12), preferentially a short chain of dp 6, whereas PvSBE1 transferred a broader distribution of chain length (dp 6–30). The chain-length distribution pattern generated by (1Na/2Nb)-II activity was very similar to that by PvSBE2 activity (Fig. 2B), indicating that the Na region of PvSBE1 has little or no effect on the overall distribution pattern. In contrast, analyses of the hybrid enzymes constructed using maize SBEs (mBE I and II) have shown that the N-terminal regions are important for the specificity of the transferred chain length. One N-terminal chimeric enzyme (mBE I-II HindIII) between mBE I and II displayed a chain-length distribution profile that was more similar to mBE I than to mBE II (Kuriki et al., 1997). This discrepancy between the data obtained from mBE I-II HindIII and (1Na/2Nb)-II could be attributed to the difference in their constructs; in other words, mBE I-II HindIII was swapped not only in the N-domain but also in a part of the barrel domain (Kuriki et al., 1997) and is similar to (1Na/1Nb)-II, which showed negligible activity in this study. Therefore, the chain-length distribution of an SBE is likely to be determined cooperatively by the N-domain and barrel domain.

2.2 Preparation and properties of the N-terminal truncated enzyme of PvSBE2

SBEs have been predicted to consist of three domains: the N-domain, $(\beta/\alpha)_8$ barrel domain, and C-domain. The Na region used for the construction of chimeric enzymes includes the whole N-domain. The secondary structure prediction program (Pred) (Jones, 1999) predicted that the Na segment of PvSBE2 has a β-sandwich structure containing seven β-sheets (β1–β7 in Fig. 3). This predicted structure was coincident with the three-dimensional structure of *E. coli* N113BE, which is an N-terminal truncated form (Abad et al., 2002). Despite the large deletion in the N-terminal region, N113BE exhibited a substrate preference and K_m value for amylose that were similar to those of the wild-type enzyme; additionally, it retained 60% of the specific activity of the wild-type enzyme (Binderup et al., 2000). The primary sequence alignment of the N-domains of PvSBE2 and the *E. coli* N113BE showed that the N-terminus of *E. coli* N113BE corresponds to a sequence of 46 amino acids downstream of the N-terminus in PvSBE2 (Fig. 3). The Pred program predicted that these 46 amino acids formed a β-strand and a helix (Fig. 3). To investigate the effect of this region on the branching enzyme activity, an expression vector was constructed to generate a truncated enzyme designated ΔN46-PvSBE2 that lacked the first 46 amino acids from its N-terminus. Although the recombinant ΔN46-PvSBE2 was found in the soluble extracts from the cells harboring the expression plasmid (Fig. 4A), ΔN46-PvSBE2 had no branching enzyme activity, indicating that the 46 amino acids are indispensable for catalysis.

Interestingly, when the soluble crude extracts from the cells were stored at 4˚C for 6 days, ΔN46-PvSBE2 was easily proteolyzed probably by endogenous proteinase(s) from the *E. coli* cells, whereas PvSBE2 remained stable (Fig. 4B), suggesting that the deletion of 46 amino acids alters the conformation of the N-domain and the overall structure.

2.3 Analysis of the site-directed mutant enzymes

The primary sequence alignment of various plant SBEs revealed that five amino acid residues in the regions corresponding to the first 46 amino acids of PvSBE2 were completely conserved (Fig. 5). In this study, to estimate the significance of these residues, we focused on the three amino acid residues (Asp-15, His-24, and Arg-28) that have positive or negative charges and then introduced site-directed mutations. Five mutant enzymes (designated D15A-, D15E-, H24A-, R28A-, and R28K-PvSBE2) were prepared by substituting Asp-15 with alanine or glutamic acid, His-24 with alanine, and Arg-28 with alanine or lysine, and were purified from the *E. coli* cells. The homogeneity of each enzyme was confirmed using a Coomassie brilliant blue-stained SDS-PAGE gel (data not shown). The specific activity of each purified enzyme was measured against amylose and compared with that of PvSBE2 under the standard assay conditions that included 0.1 M citrate (Table 1). In the three mutants in which some amino acids were replaced with alanine, D15A- and R28A-PvSBE2 displayed a specific activity that was approximately 10% of that displayed by PvSBE2; however,

H24A-PvSBE2 retained 38% of the activity of PvSBE2. When Asp-15 and Arg-28 were replaced with an acidic amino acid, glutamic acid, and a basic amino acid, lysine, respectively, D15E-PvSBE2 showed 31.3% of the specific activity of PvSBE2, whereas R28K-PvSBE2 had a specific activity that was nearly identical to that of PvSBE2.

To examine the effect of these mutations on the whole structure, the thermal stability of each site-directed mutant was determined and compared with that of PvSBE2 (Fig. 6). When the enzymes were maintained for 15 min at various temperatures ranging from 30°C to 60°C, more than 80% of the original activity was retained up to 47.5°C for PvSBE2, up to 40°C for D15A- and D15E-PvSBE2, up to 42.5°C for R28A- and H24A-PvSBE2, and up to 45°C for R28K-PvSBE2. The reduced thermostabilities of the mutant enzymes suggest that the mutations have an influence on the conformation.

The kinetics parameters of each mutant enzyme were also analyzed using amylose and compared with those obtained for PvSBE2 (Table 1). The Lineweaver–Burk plots of the reaction catalyzed by D15A-, D15E-, R28A-, R28K-, and H24A-PvSBE2 showed the K_m values for amylose to be 1.3, 1.52, 1.57, 1.55, and 1.59 mg/ml, respectively, and the V_{max} values to be 28, 73, 20, 220, and 74 U/mg, respectively. The large decreases in the specific activities of the mutants except R28K-PvSBE2 were predominantly attributed to their reduced V_{max} values. These results indicate that the mutations in the N-terminal region of PvSBE2 affect the catalytic rate but have little influence on the apparent affinity for amylose. The significant decreases in the V_{max} values and thermostabilities of D15A- and R28A-PvSBE2 suggest that Asp-15 and Arg-28 of

PvSBE2 are the key residues that help to retain the conformation essential for the enzyme activity.

3. Conclusions

The results from this study and previous reports suggest a hypothetical N-terminal structural model of PvSBE2 (Fig. 7). A comparison of the N-terminal primary sequences of SBEs from the families A and B has indicated that there is a flexible domain in some family A SBEs, such as pea SBEI, maize BEIIb, and rice RBE3. Burton et al. (1995) predicted that this domain might be involved in the interactions between SBE and starch or in determining the type of glucan chain the enzyme can utilize as a substrate. Our previous data demonstrated that the flexible domain in LF-PvSBE2—the N-terminal extension form of PvSBE2—is not essential for enzyme catalysis but contributes to the affinity for amylopectin (Hamada et al., 2002). Hence, the flexible domain in a family A SBE is structurally independent of the other domains. In contrast, an N-domain is located between the flexible and barrel domains and interacts with the catalytic barrel domain. The structural alterations in the N-domain cause a decrease in enzyme activity through the reduced interaction between the N-domain and barrel domain. In conclusion, the results in this study show for the first time that the N-terminal region of an SBE, including specific residues such as Asp-15 and Arg-28, which is not necessary for *E. coli* GBE activity, is responsible for the stable conformation of the N-domain and barrel domain, and consequently for optimal activity.

4. Experimental

4.1. Construction of plasmids for the expression of chimeric, truncated, and site-directed mutant enzymes

The construction of the expression vectors used in this study is described in detail in the supplementary data (Tables S1 and S2 and Figs. S1 and S2). All the fragments amplified by polymerase chain reaction (PCR) were sequenced to verify that no errors had occurred during polymerization. The pET-(1/1)2, pET-(1/2)2, pET-(2/1)2, pET-(1/2)1, pET-(2/1)1, and pET-(2/2)1 plasmids were constructed for the production of the chimeric enzymes (1Na/1Nb)-II, (1Na/2Nb)-II, (2Na/1Nb)-II, (1Na/2Nb)-I, (2Na/1Nb)-I, and (2Na/2Nb)-I, respectively (Fig. 1). The pET-ΔN46-PvSbe2 plasmid was prepared for the expression of the N-terminal truncated form of PvSBE2. The pET-D15A, pET-D15E, pET-H24A, pET-R28A, and pET-R28K plasmids were constructed to produce the recombinant proteins with different site-directed mutations. *E. coli* BL21 (DE3) (Novagen; Madison, WI) was transformed by each expression vector.

4.2. Expression and purification of the recombinant proteins

E. coli cells carrying each expression vector were grown in 2.4 liter of the Luria–Bertani medium containing 100 μg/ml of ampicillin at 25˚C. Cells were

induced with 0.5 mM isopropyl β-D-thiogalactoside (final concentration) at 25˚C for 10 h and were then harvested by centrifugation. All purification steps were performed at 4˚C. The following purification procedures can separate the recombinant SBEs and the endogenous GBE sufficiently.

(1) Purification of the chimeric and truncated enzymes

The chimeric and N-terminal truncated enzymes were expressed as recombinant enzymes without a His-tag. The cells were ruptured by passing the cell suspension through a French Press (Ohtake Works; Tokyo, Japan) in 20 mM Tris-HCl buffer (pH 7.5) containing 50 mM NaCl, 1 mM EDTA, and 1 mM dithiothreitol (DTT). After centrifugation, the supernatant (crude extract) was dialyzed against a buffer (20 mM Tris-HCl, pH 7.5, 1 mM EDTA, and 1 mM DTT) and then subjected to enzyme purification by three column chromatography steps using DEAE-Sepharose CL-6B (GE Healthcare Bio-Sciences Corp.; Piscataway, NJ), Bio-Gel P-200 (Bio-Rad Laboratories Inc.; Tokyo, Japan), and Gigapite (Seikagaku Corp.; Tokyo, Japan) following the previous purification procedure for PvSBE2 (Hamada et al., 2001).

(2) Purification of site-directed mutant enzymes

The cells were ruptured by a French press in buffer A (20 mM phosphate buffer, pH 7.8 containing 50 mM imidazole and 500 mM NaCl). After centrifugation, the supernatant (crude extract) was used as a crude enzyme and then applied to a chelating Sepharose FF column (1.5 cm x 5.5 cm; GE Healthcare Bio-Sciences) previously

charged with nickel ions and equilibrated with buffer A. The column was washed with buffer A, and then proteins with a His-tag were eluted with a gradient of 50–300 mM imidazol. The active fractions were pooled and dialyzed against buffer B (20 mM Tris-HCl buffer, pH 6.8, containing 1 mM EDTA and 1 mM DTT) and then fractionated on a DEAE-Sepharose CL-6B column (1.8 cm x 11.5 cm, GE Healthcare Bio-Sciences) equilibrated with buffer B. The column was washed with buffer B followed by elution with a gradient of 0–0.5 M NaCl. The active fractions were pooled and used for further study as a purified enzyme. The purity of the enzymes was determined by SDS-PAGE followed by staining with a Coomassie brilliant blue (Laemmli, 1970).

4.3. Assay of SBE activity

SBE activity was measured by the following assays, as described previously.

Assay I. The iodine-staining assay was performed by monitoring the decrease in absorbance at 660 nm for amylose (potato amylose type III, Sigma-Aldrich; St. Louis, MO), as described by Boyer and Preiss (1978). One unit of enzyme activity was defined as the amount of enzyme yielding a decrease in A_{660} of 0.1 per minute at 30˚C.

Assay BL. The branching linkage assay determines the number of branching linkages introduced into the substrate, i.e., reduced amylose, and was performed by the methods of Takeda et al. (1993). One unit of enzyme activity was defined as the amount of enzyme forming 1 μmol of branch linkages per minute at 30˚C.

4.4. Enzymatic properties

The kinetics parameters and temperature stability of the purified mutant enzymes were examined as described previously (Nozaki et al., 2001).

4.5. Analysis of chain transfer patterns

The chain transfer patterns were determined according to the method of Hanashiro et al. (1996). The branched products were generated by incubating the reduced amylose with 1 mU (determined by assay BL) of enzyme in 500 μl of 25 mM MOPS (pH 7.5) at 30˚C for 4 h. After the termination of the branching reactions by boiling, debranching was performed by incubation with isoamylase, as explained previously. The distribution of the transferred chain length was analyzed with an HPAEC–PAD according to the method of Tomlinson et al. (1997).

Acknowledgments

This work was supported by grants-in-aid for Scientific Research (C) (13660071, 16580069, and 18580086) and the Akiyama Foundation to HI from the Japan Society for the Promotion of Science, and a grant-in-aid for Young Scientists (B) (18780067) to SH from the Ministry of Education, Science, Sports, and Culture, Japan.

References

Abad, M.C., Binderup, K., Rios-Steiner, J., Arni, R.K., Preiss, J., Geiger, J.H., 2002. The X-ray crystallographic structure of *Escherichia coli* branching enzyme. J. Biol. Chem. 277, 42164-42170.

Baba, T., Kimura, K., Mizuno, K., Etoh, H., Ishida, Y., Shida, O., Arai, Y., 1991. Sequence conservation of the catalytic regions of amylolytic enzymes in maize branching enzyme-I. Biochem. Biophys. Res. Commun. 181, 87-94.

Binderup, K., Mikkelsen, R., Preiss, J., 2000. Limited proteolysis of branching enzyme from *Escherichia coli*. Arch. Biochem. Biophys. 377, 366-371.

Borovsky, D., Smith, E.E., Whelan, W.J., 1976. On the mechanism of amylose branching by potato Q-enzyme. Eur. J. Biochem. 62, 307-312.

Boyer, C.D., Preiss, J., 1978. Multiple forms of (1→4)-α-D-glucan, (1→4)-α-D-glucan-6-glycosyl transferase from developing *Zea mays* L. kernels. Carbohydr. Res. 61, 321-334.

Burton, R.A., Bewley, J.D., Smith, A.M., Bhattacharyya, M.K., Tatge, H., Ring, S., Bull, V., Hamilton, W.D.O., Martin, C., 1995. Starch branching enzymes

belonging to distinct enzyme families are differentially expressed during pea embryo development. Plant J. 7, 3-15.

Edwards, A., Borthakur, A., Bornemann, S., Venail, J., Denyer, K., Waite, D., Fulton, D., Smith A., Martin, C., 1999. Specificity of starch synthase isoforms from potato. Eur. J. Biochem. 266, 724-736.

Hamada, S., Ito, H., Hiraga, S., Inagaki, K., Nozaki, K., Isono, N., Yoshimoto, Y., Takeda, Y., Matsui, H., 2002. Differential characteristics and subcellular localization of two starch-branching enzyme isoforms encoded by a single gene in *Phaseolus vulgaris* L. J. Biol. Chem. 277, 16538-16546.

Hamada, S., Nozaki, K., Ito, H., Yoshimoto, Y., Yoshida, H., Hiraga, S., Onodera, S., Honma, M., Takeda, Y., Matsui, H., 2001. Two starch-branching-enzyme isoforms occur in different fractions of developing seeds of kidney bean. Biochem. J. 359, 23-34.

Hanashiro, I., Abe, J., Hizukuri, S., 1996. A periodic distribution of the chain length of amylopectin as revealed by high-performance anion-exchange chromatography. Carbohydr. Res. 283, 151-159.

Hong, S., Mikkelsen, R., Preiss, J., 2001. Analysis of the amino terminus of maize

branching enzyme II by polymerase chain reaction random mutagenesis. Arch. Biochem. Biophys. 386, 62-68.

Hong, S., Preiss, J., 2000. Localization of C-terminal domains required for the maximal activity or for determination of substrate preference of maize branching enzymes. Arch. Biochem. Biophys. 378, 349-355.

Ito, H., Hamada, S., Isono, N., Yoshizaki, T., Ueno, H., Yoshimoto, Y., Takeda, Y., Matsui, H., 2004. Functional characteristics of C-terminal regions of starch-branching enzymes from developing seeds of kidney bean (*Phaseolus vulgaris* L.). Plant Sci. 166, 1149-1158.

Jones, D.T., 1999. Protein secondary structure prediction based on position-specific scoring matrices. J. Mol. Biol. 292, 195-202.

Koßmann, J., Visser, R.G.F., Müller-Röber, B., Willmitzer, L., Sonnewald, U., 1991. Cloning and expression analysis of a potato cDNA that encodes branching enzyme: evidence for co-expression of starch biosynthetic genes. Mol. Gen. Genet. 230, 39-44.

Kuriki, T., Imanaka, T., 1999. The concept of the α-amylase family: Structural similarity and common catalytic mechanism. J. Biosci. Bioeng. 87, 557-565.

Kuriki, T., Stewart, D.C., Preiss, J., 1997. Construction of chimeric enzymes out of maize endosperm branching enzymes I and II: activity and properties. J. Biol. Chem. 272, 28999-29004.

Laemmli, U.K., 1970. Cleavage of structural proteins during the assembly of the head of bacteriophage T4. Nature 227, 680-685.

Manners, D.J., 1989. Recent developments in our understanding of amylopectin structure. Carbohydr. Polym. 11, 87-112.

Mizuno, K., Kawasaki, T., Shimada, H., Satoh, H., Kobayashi, E., Okumura, S., Arai, Y., Baba, T., 1993. Alteration of the structural properties of starch components by the lack of an isoform of starch branching enzyme in rice seeds. J. Biol. Chem. 268, 19084-19091.

Nagamine, T., Yoshida, H., Komae, K., 1997. Varietal differences and chromosome locations of multiple isoforms of starch branching enzyme in wheat endosperm. Phytochemistry 46, 23-26.

Nakamura, Y., Takeichi, T., Kawaguchi, K., Yamanouchi, H., 1992. Purification of two forms of starch branching enzyme (Q-enzyme) from developing rice endosperm.

Physiol. Plant. 84, 329-335.

Nozaki, K., Hamada, S., Nakamori, T., Ito, H., Sagisaka, S., Yoshida, H., Takeda, Y., Honma, M., Matsui, H., 2001. Major isoforms of starch branching enzymes in premature seeds of kidney bean (*Phaseolus vulgaris* L.). Biosci. Biotech. Biochem. 65, 1141-1148.

Poulsen, P., Kreiberg, J.D., 1993. Starch branching enzyme cDNA from *Solanum tuberosum*. Plant Physiol. 102, 1053-1054.

Romeo, T., Kumar, A., Preiss, J., 1988. Analysis of the *Escherichia coli* glycogen gene cluster suggests that catabolic enzymes are encoded among the biosynthetic genes. Gene 70, 363-376.

Smith, A.M., 1988. Major differences in isoforms of starch-branching enzyme between developing embryos of round- and wrinkled-seeded peas (*Pisum sativum* L.). Planta 175, 270-279.

Svensson, B., 1994. Protein engineering in the α-amylase family: catalytic mechanism, substrate specificity, and stability. Plant Mol. Biol. 25, 141-157.

Takata, H., Kuriki, T., Okada, S., Takesada, Y., Iizuka, M., Minamiura, N., Imanaka, T.,

1992. Action of neopullulanase. Neopullulanase catalyzes both hydrolysis and transglycosylation at α-(1→4)- and α-(1→6)-glucosidic linkages. J. Biol. Chem. 267, 18447-18452.

Takeda, Y., Guan, H-P., Preiss, J., 1993. Branching of amylose by the branching isoenzymes of maize endosperm. Carbohydr. Res. 240, 253-263.

Tomlinson, K.L., Lloyd, J.R., Smith, A.M., 1997. Importance of isoforms of starch-branching enzyme in determining the structure of starch in pea leaves. Plant J. 11, 31-43.

Figure legends

Fig. 1. Schematic diagram representing mature PvSBE1 and PvSBE2 and the constructed N-terminal chimeric enzymes. Mature PvSBE1 and PvSBE2 are shown in white and gray, respectively. The numbers I–IV in the central portion denote the four conserved regions among the enzymes of the α-amylase family. The broken lines show the borders between the barrel domain and N-domain and those between the barrel domain and C-domain. The numbers of amino acids indicate the residues in each region. The triangles show the displacement sites for the construction of each region from PvSBE1 and PvSBE2. The distal and proximal halves of the substituted regions are labeled as Na and Nb regions, respectively. The C-domain and a part of the barrel domain containing the four conserved regions are designated as the basic core structural region. Each chimeric enzyme was named based on the origins of the three different regions; for example, (2Na/1Nb)-I indicates the name of the enzyme containing the Na region from PvSBE2, Nb region from PvSBE1, and basic core structural region from PvSBE1. Specific activities in each crude extract are expressed as U/mg of protein measured by the assay I. BL21(DE3) with pET23d refers to endogenous glycogen-branching enzyme activity.

Fig. 2. Effects of citrate and chain-transfer pattern analysis of (1Na/2Nb)-II. The data for PvSBE1 and PvSBE2 are cited from the previous paper (Hamada et al., 2001) for comparison. (A) Enzyme activity of PvSBE1 (open squares), PvSBE2 (open

circles), and (1Na/2Nb)-II (closed circles) are shown relative to the original activity without citrate (100%). (B) Analysis was carried out as described in the text following the incubation of the reduced amylose with PvSBE1, PvSBE2, or (1Na/2Nb)-II and the subsequent incubation with isoamylase. Debranched α-glucan was analyzed by HPAEC–PAD.

Fig. 3. Sequence alignment and secondary structure prediction of the N-domain between PvSBE2 and *E. coli* N113BE. The following sequences were obtained from the GenBank/EMBL/DDBJ databases: PvSBE1 and PvSBE2 from *Phaseolus vulgaris* L. (**AB029549** and **AB029548**) and *E. coli* GBE (**M13751**). The elements of the secondary structure of the glycogen-branching enzyme from *E. coli* elucidated in the X-ray structure (Abad et al., 2002) appear above the sequence. The secondary structure of PvSBE2 predicted by the Pred (Jones, 1999) program is shown below the sequence.

Fig. 4. SDS-PAGE and immunoblot analysis of the N-terminal truncated PvSBE2 (ΔN46-PvSBE2). (A) CBB-stained SDS-PAGE gel (upper) and immunoblot detected using an anti-PvSBE2 (lower). Lane T was loaded with total cell extraction. Lanes Sup. and Ppt. contain the supernatant and precipitate, respectively, that were obtained after rupturing the cells in a French press. (B) Immunoblot detection of the stored samples with anti-PvSBE2. The two lanes on the left were loaded with the supernatant fraction immediately after the rupture of the cells, and the two lanes on the right

contained the supernatant after preserving at 4˚C for 6 days.

Fig. 5. Sequence alignment of branching enzymes from various organisms. The conserved amino acid residues among all SBEs are boxed. The asterisks above the PvSBE2 sequence indicate the amino acids that were subjected to site-directed mutagenesis in this study. The secondary structural elements are shown above the aligned sequences. The following sequences were obtained from the GenBank/EMBL/DDBJ databases: PvSBE1 and PvSBE2 from *Phaseolus vulgaris* L. (**AB029549** and **AB029548**); pea SBEI and SBEII from *Pisum sativum* L. (**X80009** and **X80010**); rice SBE1, SBE3, and SBE4 from *Oryza sativa* L. (**AY302112**, **D16201** and **AB023498**); maize BEI, BEIIa, and BEIIb from *Zea mays* L. (**U17897**, **U65948** and **L08065**); wheat SBEI and SBEII from *Triticum aestivum* L. (**Y12320** and **Y11282**); barley BEIIa and IIb from *Hordeum vulgare* L. (**AF064560** and **AF064561**); ArabBE2.1 and 2.2 from *Arabidopsis thaliana* (**AK226896** and **U22428**); and potato SBEI and SBEII from *Solanum tuberosum* L. (**X69805** and **AJ011888**).

Fig. 6. Heat stability of the mature PvSBE2 and site-directed mutant enzymes. Samples were heated to the indicated temperatures for 15 min followed by cooling on ice for 5 min. The remaining activity was determined by assay I. The activity at 30˚C was set to 100%.

Fig. 7. A model for the role of the N-domain in enzyme stability and optimal activity.

The flexible domain (broken circle) is structurally independent with respect to the other domains. In SBEs, the N-domain contains a β-strand and a helix and interacts closely with the catalytic barrel domain. The thicknesses of the two-headed open arrows indicate the strengths of interactions between these domains. The conformational changes in the N-domain by chimera formation, deletion, or site-directed mutations influence the activity and total stability.

Table 1

Kinetic parameters and specific activities of the chimeric, N-terminal truncated, and site-directed mutant enzymes for amylose

Enzyme	K_m[b] (mg/ml)	V_{max}[b] (U/mg protein)	Specific activity (U/mg protein) Citrate		
			0 M	0.1 M	(%)
PvSBE1 [a]	0.46	320	219	254	
PvSBE2 [a]	1.27	242	107	214	(100)
(1Na/2Nb)-II	0.63	10	6.1	13	(6.1)
D15A-PvSBE2	1.30	28	12.3	28	(13.1)
D15E-PvSBE2	1.52	73	32.9	67	(31.3)
R28A-PvSBE2	1.57	20	7.8	23	(10.7)
R28K-PvSBE2	1.55	220	86	200	(93.5)
H24A-PvSBE2	1.59	74	28.5	82	(38.3)

[a] The data for PvSBE1 and PvSBE2 are cited from our previous paper (Hamada et al., 2001).

[b] These values were calculated using double reciprocal plots described in the supplementary Fig. S3.

Figure 1. Hamada et al.

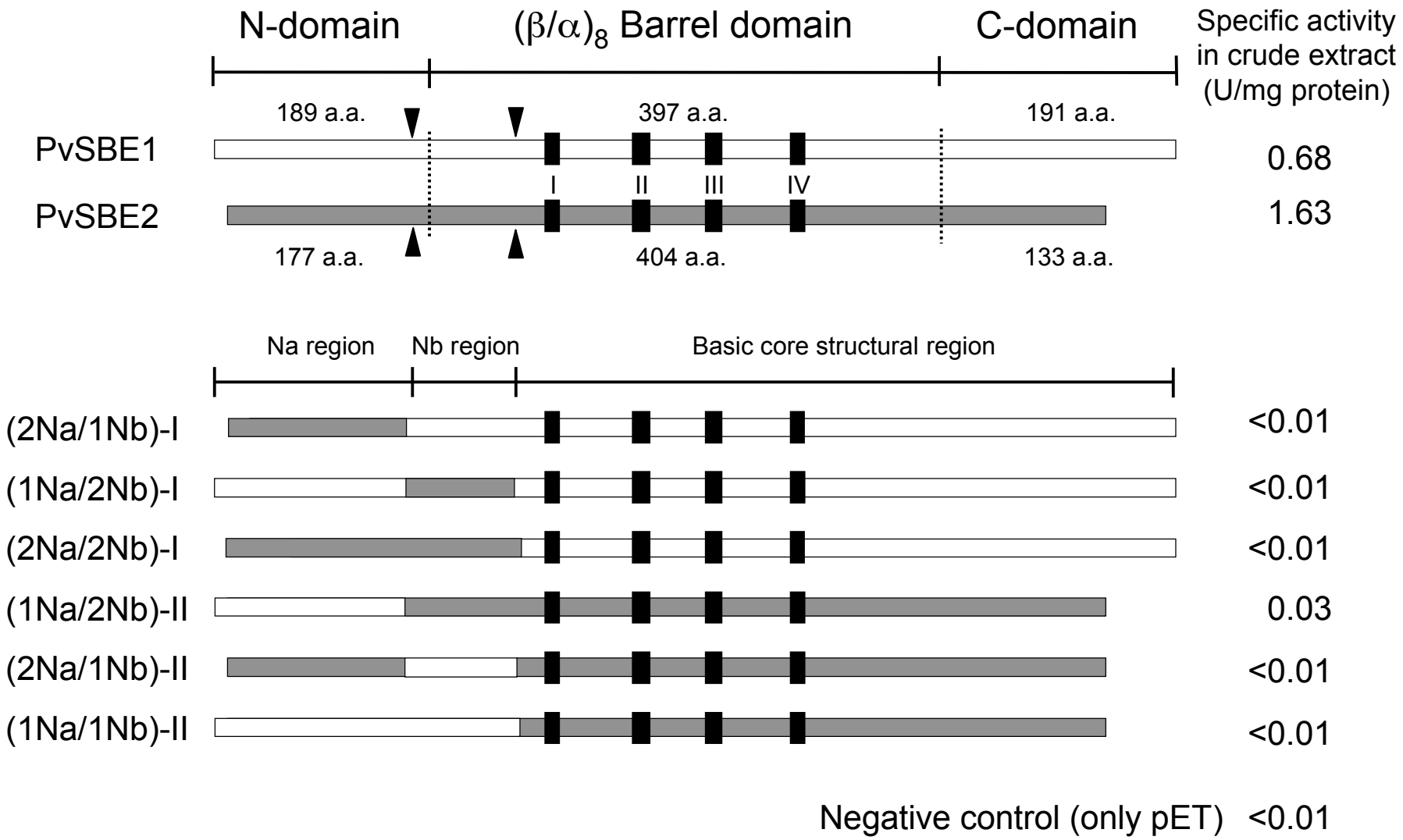

Figure 2. Hamada et al.

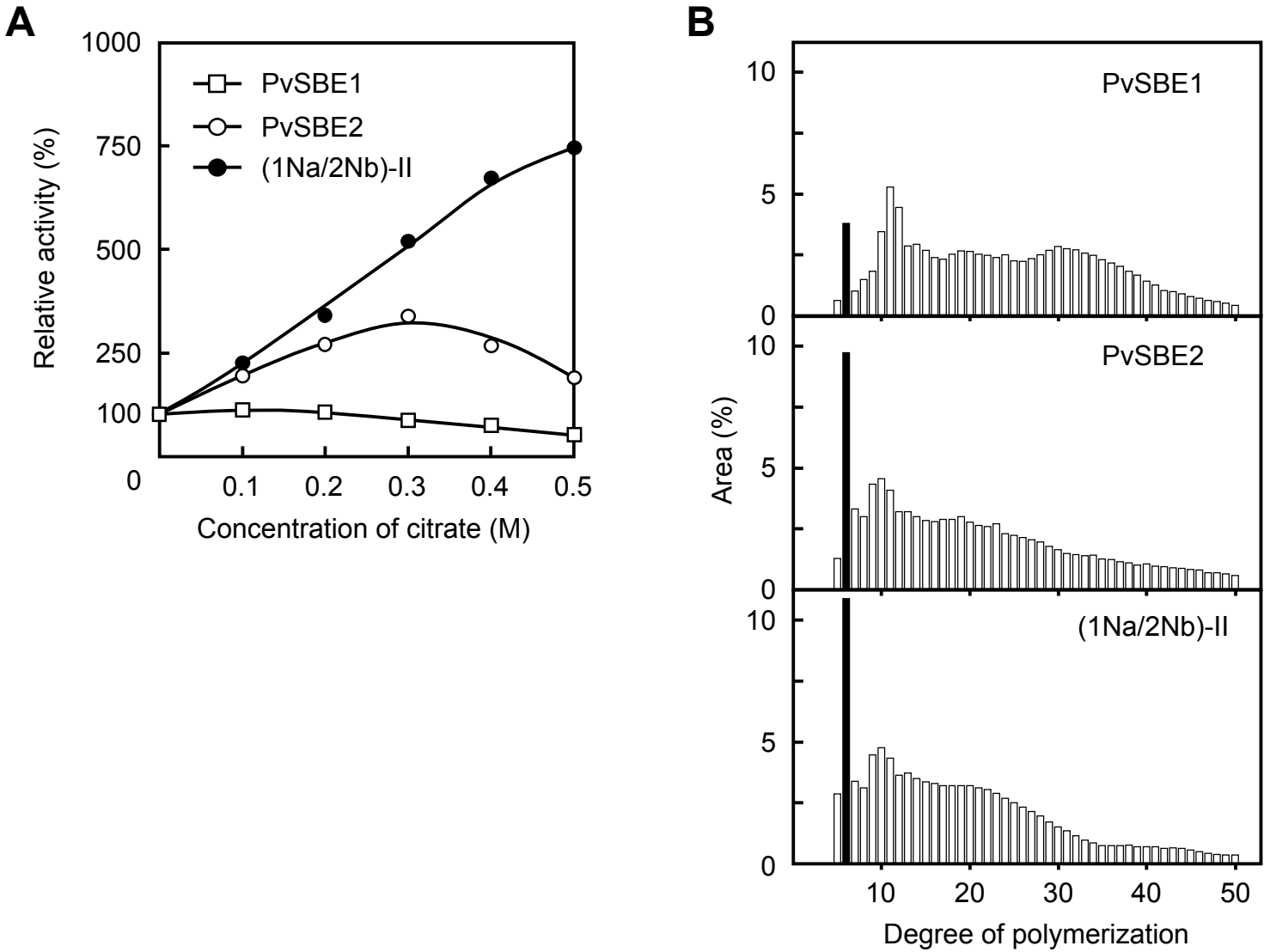

Figure 3. Hamada et al.

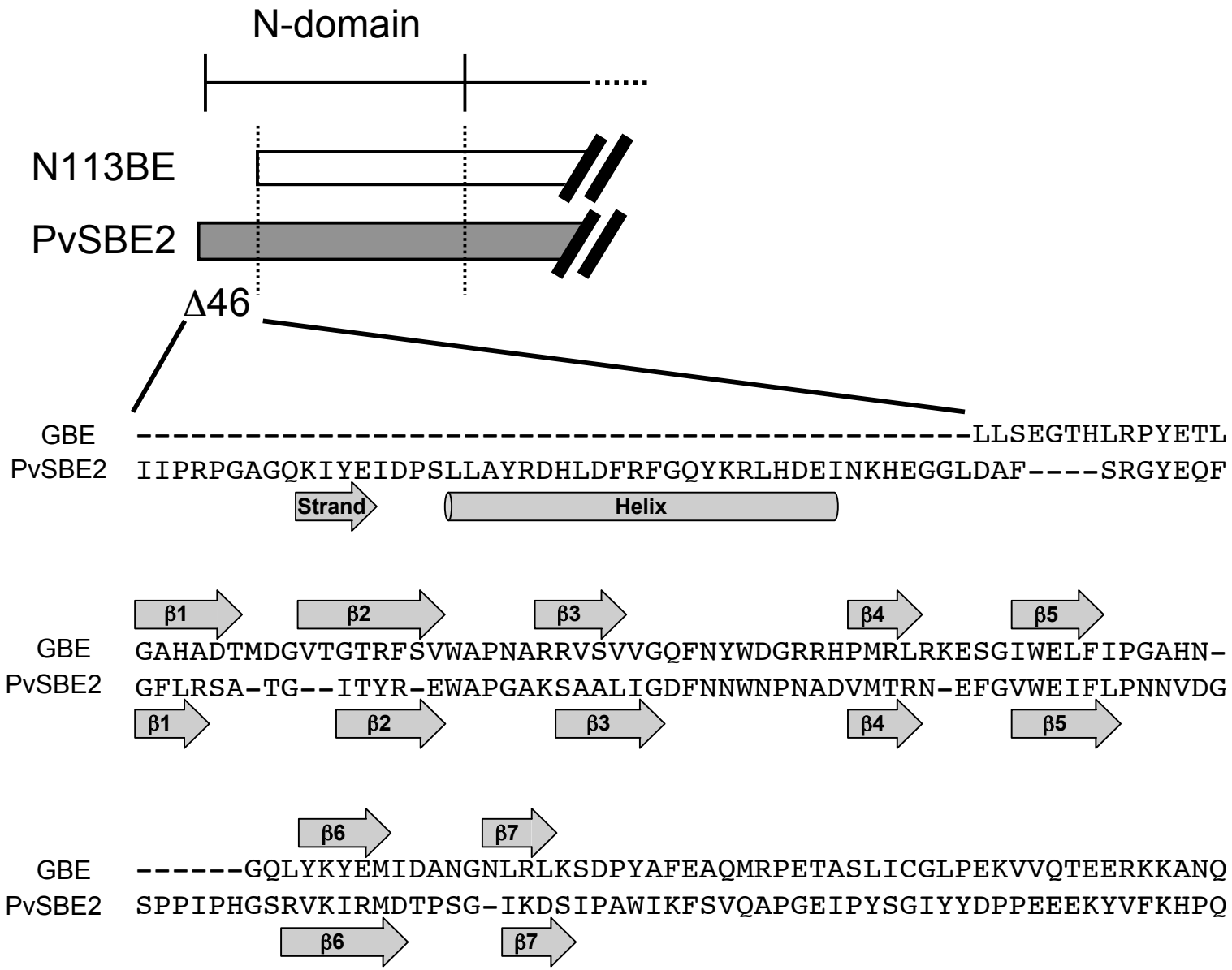

Figure 4. Hamada et al.

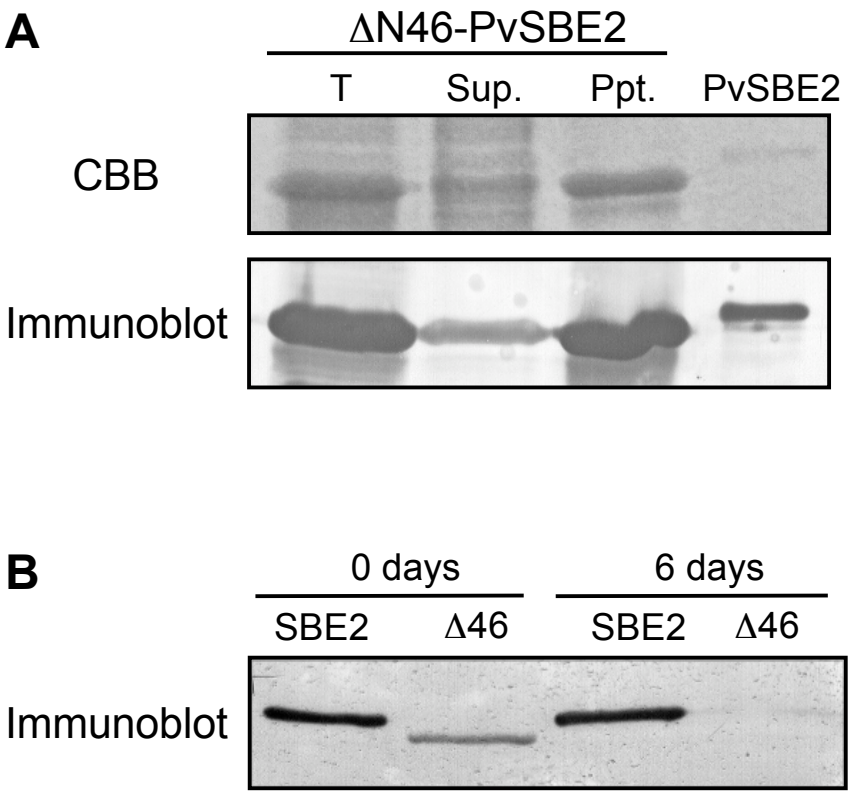

Figure 5. Hamada et al.

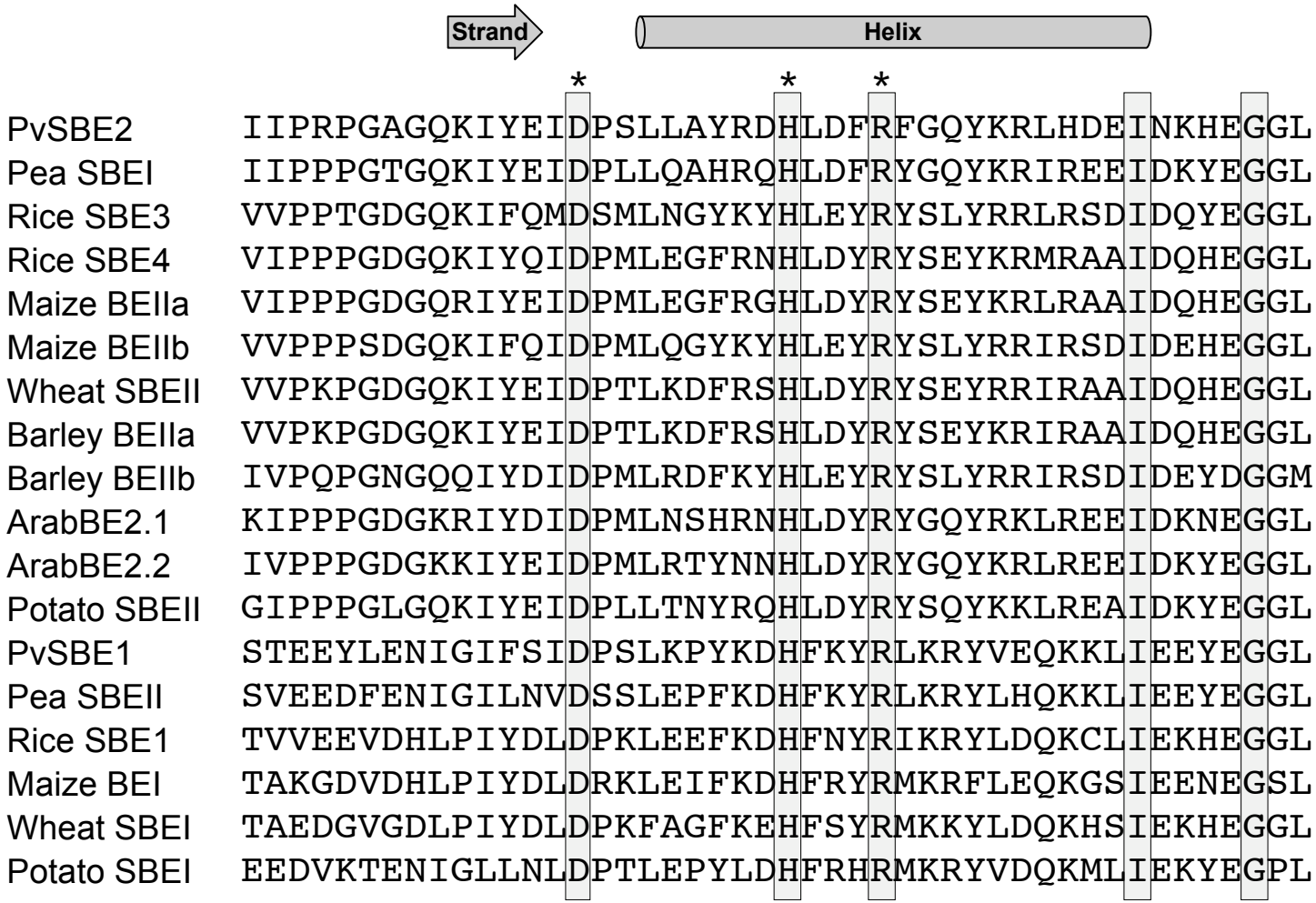

Figure 6. Hamada et al.

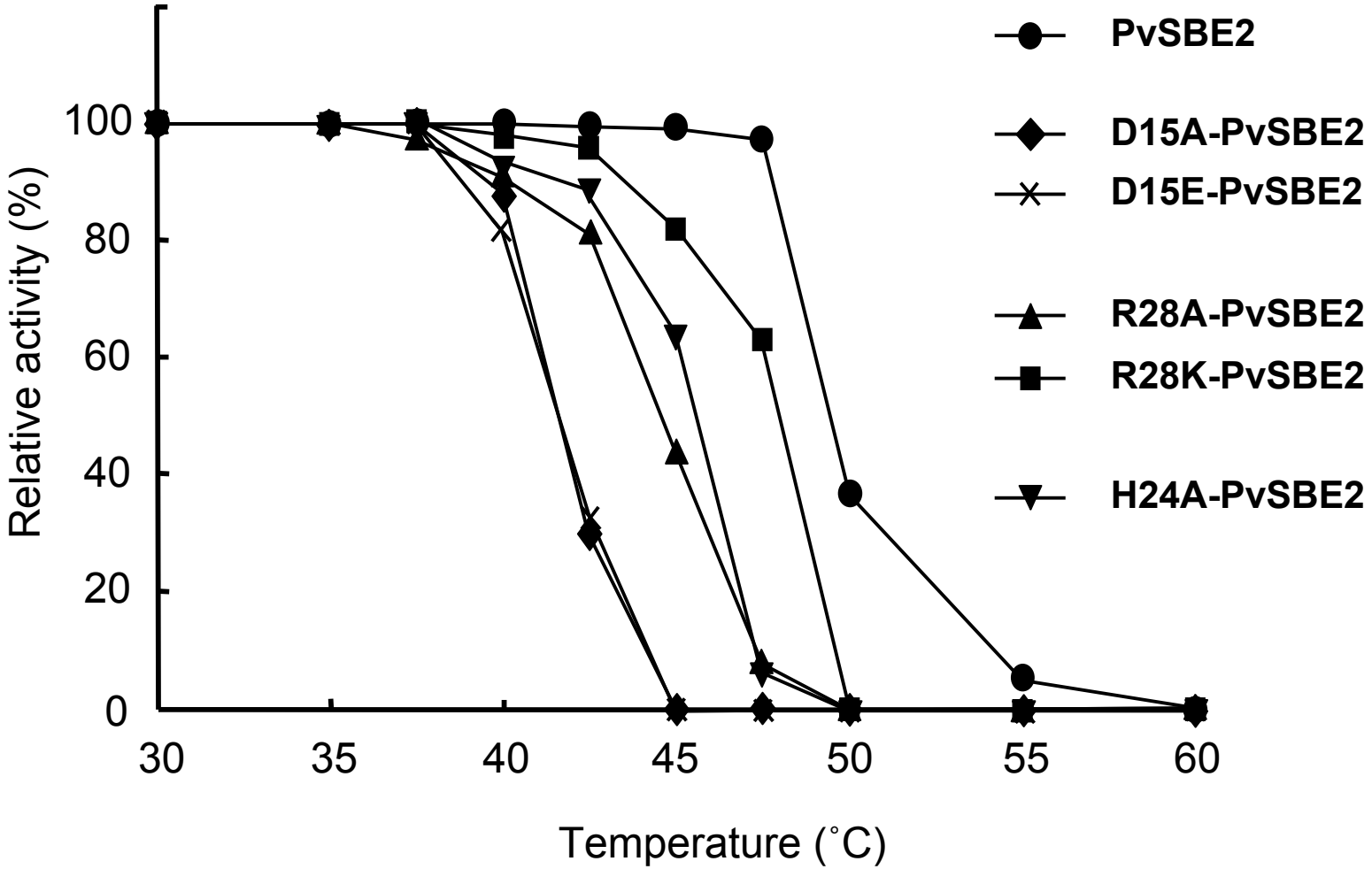

Figure 7. Hamada et al.

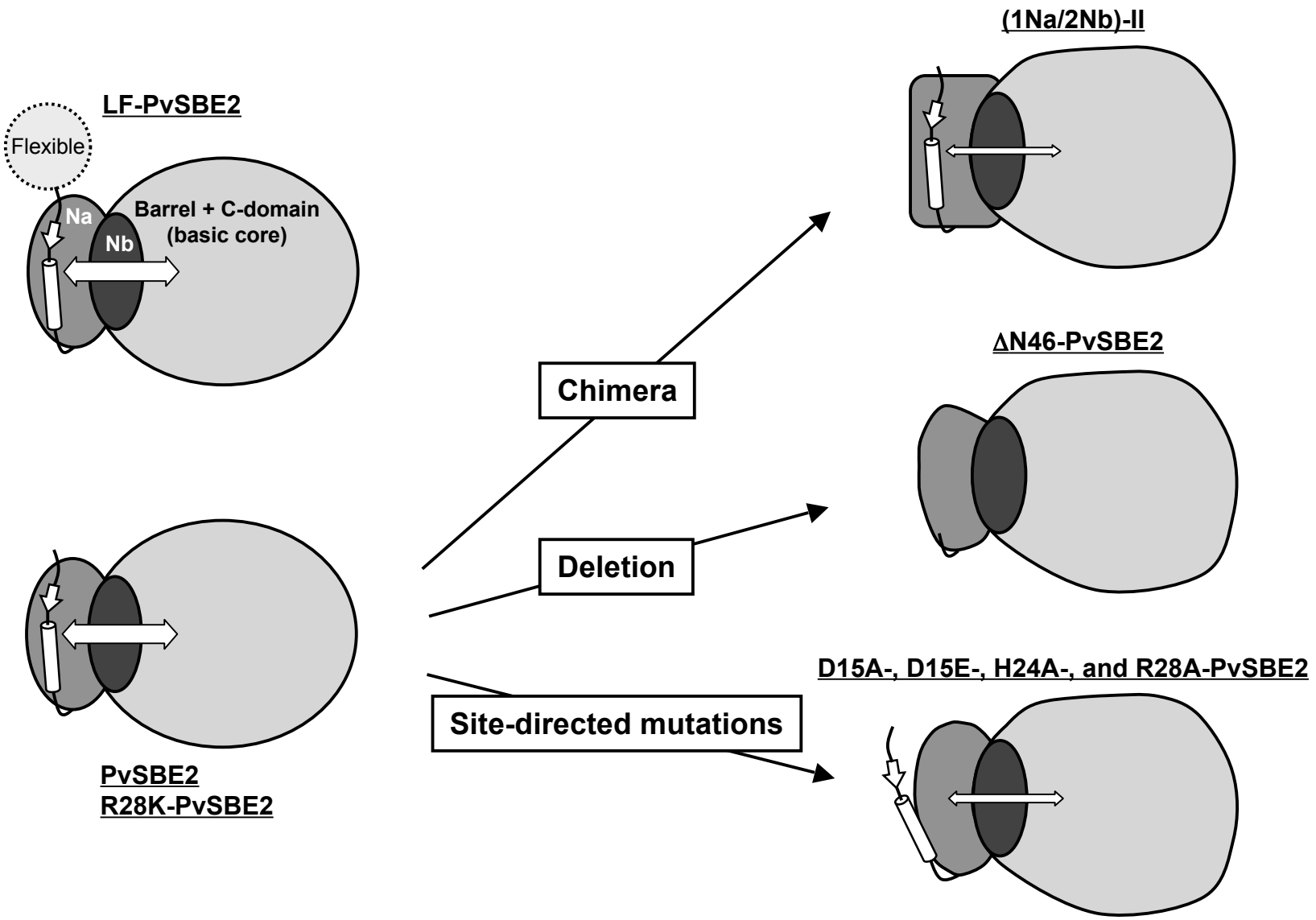

Supplementary Data

S1. Experimental

S1.1. Oligonucleotides and PCR reaction

The oligonucleotides used in this study are listed in the supplementary Table S1. Each PCR reaction and amplified fragment is shown in Table S2.

S1.2. Construction of chimeric enzymes

Each SBE DNA fragment used for constructing expression vectors was prepared by the overlap extension method using PCR, as described previously (Ito et al., 2004) (Fig. S1). PCR was performed using LA Taq polymerase (TaKaRa Bio Inc., Kyoto, Japan), and all amplified fragments were sequenced to confirm that no error had occurred during polymerization. Each fragment of the chimeric region was replaced using the *Nco*I and *Kpn*I sites in the pET-PvSbe1 and pET-PvSbe2 plasmids (Hamada et al., 2001). By performing a PCR reaction, a new *Kpn*I site (silent mutation) was created, and the original *Nco*I (silent mutation) was deleted in the pET-PvSbe1 plasmid.

The construction of the pET-(1/1)2, pET-(1/2)2, and pET-(2/1)2 plasmids was accomplished by the insertion of *Nco*I/*Kpn*I-(1Na/1Nb), *Nco*I/*Kpn*I-(1Na/2Nb), and *Nco*I/*Kpn*I-(2Na/1Nb) fragments, respectively, into the *Nco*I/*Kpn*I-pET-PvSbe2 plasmid

(Fig. S1 (1)–(3)). The chimeric enzymes, which were produced by the *E. coli* cells harboring pET-(1/1)2, pET-(1/2)2, and pET-(2/1)2, were designated as (1Na/1Nb)-II, (1Na/2Nb)-II, and (2Na/1Nb)-II, respectively. The pET-(1/2)1, pET-(2/1)1, and pET-(2/2)1 plasmids were constructed by the ligation of *Nco*I/*Kpn*I-(1Na/2Nb), *Nco*I/*Kpn*I-(2Na/1Nb), and *Nco*I/*Kpn*I-(2Na/2Nb) fragments, respectively, with the *Kpn*I/*EcoR*I-PvSBE1 core region incorporated into pET23d (Fig. S1 (4)–(6)). The chimeric enzymes, which were produced by the *E. coli* cells harboring the pET-(1/2)1, pET-(2/1)1, and pET-(2/2)1 plasmids, were designated (1Na/2Nb)-I, (2Na/1Nb)-I, and (2Na/2Nb)-I, respectively.

S1.3. Construction of the N-terminal truncated enzyme

The ΔN46 fragment amplified by PCR (supplementary Table S2) was digested with *Nco*I and *Kpn*I and substituted for the *Nco*I/*Kpn*I fragment of the pET-PvSbe2 plasmid to yield the pET-ΔN46-PvSbe2 plasmid (supplementary Fig. S1 (7)). The N-terminal truncated enzyme of PvSBE2 that is produced by the *E. coli* cells carrying this plasmid was designated ΔN46-PvSBE2.

S1.4. Site-directed mutagenesis of the N-terminal region

(1) The pET-PvSbe2:His plasmid (supplementary Fig. S2 (1)) was constructed for the expression of the mature PvSBE2 with a hexahistidine tag at the C-terminus. The

amplified SBE2-C fragment (supplementary Table S2) was digested with *Eco*RV and *Xho*I and then cloned into the corresponding sites of pET-PvSbe2 (Hamada et al., 2001).

(2) The *Pvu*II/*Nhe*I-D15A and *Pvu*II/*Nhe*I-D15E fragments containing site-directed mutations (Tables S1 and S2) were substituted for the *Pvu*II/*Nhe*I fragment of the pET-PvSbe2:His plasmid to yield pET-D15A and pET-D15E (Fig. S2 (2)).

(3) The mutated H24A fragment (Tables S1 and S2) was digested with *Nhe*I and *Kpn*I and cloned into the corresponding sites of pET-PvSbe2:His to generate pET-H24A (Fig. S2 (3)).

(4) The R28A and R28K fragments (Tables S1 and S2) were prepared from the pBS-PvSbe2 plasmids in which mutations were introduced using the Transformer^{TM} Site-Directed Mutagenesis Kit 2nd version (BD Bioscience Clontech; Mountain View, CA) (Deng and Nickoloff, 1992) and were substituted for the *Nhe*I/*Kpn*I fragment of the pET-PvSbe2:His plasmid to construct pET-R28A and pET-R28K (Fig. S2 (4)).

The recombinant enzymes produced by the *E. coli* cells carrying the pET-D15A, pET-D15E, pET-H24A, pET-R28A, and pET-R28K plasmids were designated D15A-, D15E-, H24A-, R28A-, and R28K-PvSBE2, respectively.

References

Deng, W.P., Nickoloff, J.A., 1992. Site-directed mutagenesis of virtually any plasmid by eliminating a unique site. Anal. Biochem. 200, 81-88.

Hamada, S., Nozaki, K., Ito, H., Yoshimoto, Y., Yoshida, H., Hiraga, S., Onodera, S., Honma, M., Takeda, Y., Matsui, H., 2001. Two starch-branching-enzyme isoforms occur in different fractions of developing seeds of kidney bean. Biochem. J. 359, 23-34.

Ito, H., Hamada, S., Isono, N., Yoshizaki, T., Ueno, H., Yoshimoto, Y., Takeda, Y., Matsui, H., 2004. Functional characteristics of C-terminal regions of starch-branching enzymes from developing seeds of kidney bean (*Phaseolus vulgaris* L.). Plant Sci. 166, 1149-1158.

Supplementary Table S1

Oligonucleotide primer sequences used to construct chimeric, N-terminal truncated, and site-directed mutant enzymes

Primers	Sequence (5' to 3')	Position in pvsbe1 and pvsbe2 cDNA
#1	GTTTCAAGGGTGCCATGGTTATGACAGATG	255-284 (pvsbe1)
#2	CTCCATCCCCATGTCGGAATCTAAAC	689-664 (pvsbe1)
#3	GTTTAGATTCCGACATGGGGATGGAG	664-689 (pvsbe1)
#4	GCATAGAATTCTGTCACATGGTACCCAAATG	1020-990 (pvsbe1)/1313-1283 (pvsbe2)
#5	ATTTGATCCACGCCGGGATGCGATCAAC	755-695 (pvsbe1)
#6	CATCCCGGCGTGGATCAAATTTTCTGTAC	1002-1030 (pvsbe2)
#7	CATCCCGGCGTGGATCAAATATGCC	703-727 (pvsbe1)
#8	GCTAAACCCATGGTCATACCCCGAG	589-613 (pvsbe2)
#9	ATTTGAACCACGCCGGGATGGAGTCTTTGATTC	1021-989 (pvsbe2)
#10	CATTTGGGTACCATGTGACAAACTTTTATGC	990-1020 (pvsbe1)
#T7	GTAATACGACTCACTATAGGGC	625-646 (pBluescript II SK)
#11	AAGGTGCCATGGATGCATTTTCTCGG	728-753 (pvsbe2)
#12	GACTTAGGATCCTCTGGGGTTCC	1352-1330 (pvsbe2)
#His-S	GTTGGTGACAAGACAATTGCATTT	1990-2013 (pvsbe2)
#His-A	TTCCTCGAGAGGATCAACTGGCTCTGGTT	2751-2723 (pvsbe2)
#PvuII	GCGAGGCAGCTGCGGTAAAG	985-966 (pET-23d)
#D15A	CATGCAAAGATGGAGCAATCTCATATATTTTCTG	658-625 (pvsbe2)
#D15E	CATGCAAAGATGGTTCAATCTCATATATTTTCTG	658-625 (pvsbe2)
#H24A	GCTAGCCTATCGTGACGCTCTTGA	654-677 (pvsbe2)
#R28A	GTATTGTCCAAAAGCGAAATCAAGATG	696-670 (pvsbe2)
#R28K	GTATTGTCCAAATTTGAAATCAAGATG	696-670 (pvsbe2)
#SKS	GTGACTGGTGAATATTCAACCAAGTC	2514-2539 (pBluescript II SK)

Supplementary Table S2

PCR amplification of each fragment to construct expression vectors

Template	Primers	Amplified fragment
For the preparation of 1Na/1Nb fragment		
pBS-PvSbe1	#1 and #2	#1/2 for absence of *Nco*I site
pBS-PvSbe1	#3 and #4	#3/4 for creation of *Kpn*I site
#1/2 and #3/4 fragments	#1 and #4	1Na/1Nb
For the preparation of 2Na/2Nb fragment		
pBS-PvSbe2	#8 and #4	2Na/2Nb
For the preparation of 1Na/2Nb fragment		
pBS-PvSbe1	#1 and #5	1Na
pBS-PvSbe2	#6 and #4	2Nb
1Na and 2Nb fragments	#1 and #4	1Na/2Nb
For the preparation of 2Na/1Nb fragment		
pBS-PvSbe2	#8 and #9	2Na
pBS-PvSbe1	#7 and #4	1Nb
2Na and 1Nb fragments	#8 and #4	2Na/1Nb
For the preparation of PvSBE1 core domain		
pBS-PvSbe1	#10 and #T7	For creation of *Kpn*I site
For the preparation of ΔN46 fragment		
1Na/1Nb fragment	#11 and #12	ΔN46
For the preparation of SBE2-C fragment		
pET-PvSbe2	#His-S and #His-A	SBE2-C
For the preparation of D15A and D15E fragments		
pBS-PvSbe2	#PvuII and #D15A	D15A
pBS-PvSbe2	#PvuII and #D15E	D15E
For the preparation of H24 fragment		
pBS-PvSbe2	#H24A and #12	H24A

Figure S1 (1). Hamada et al.

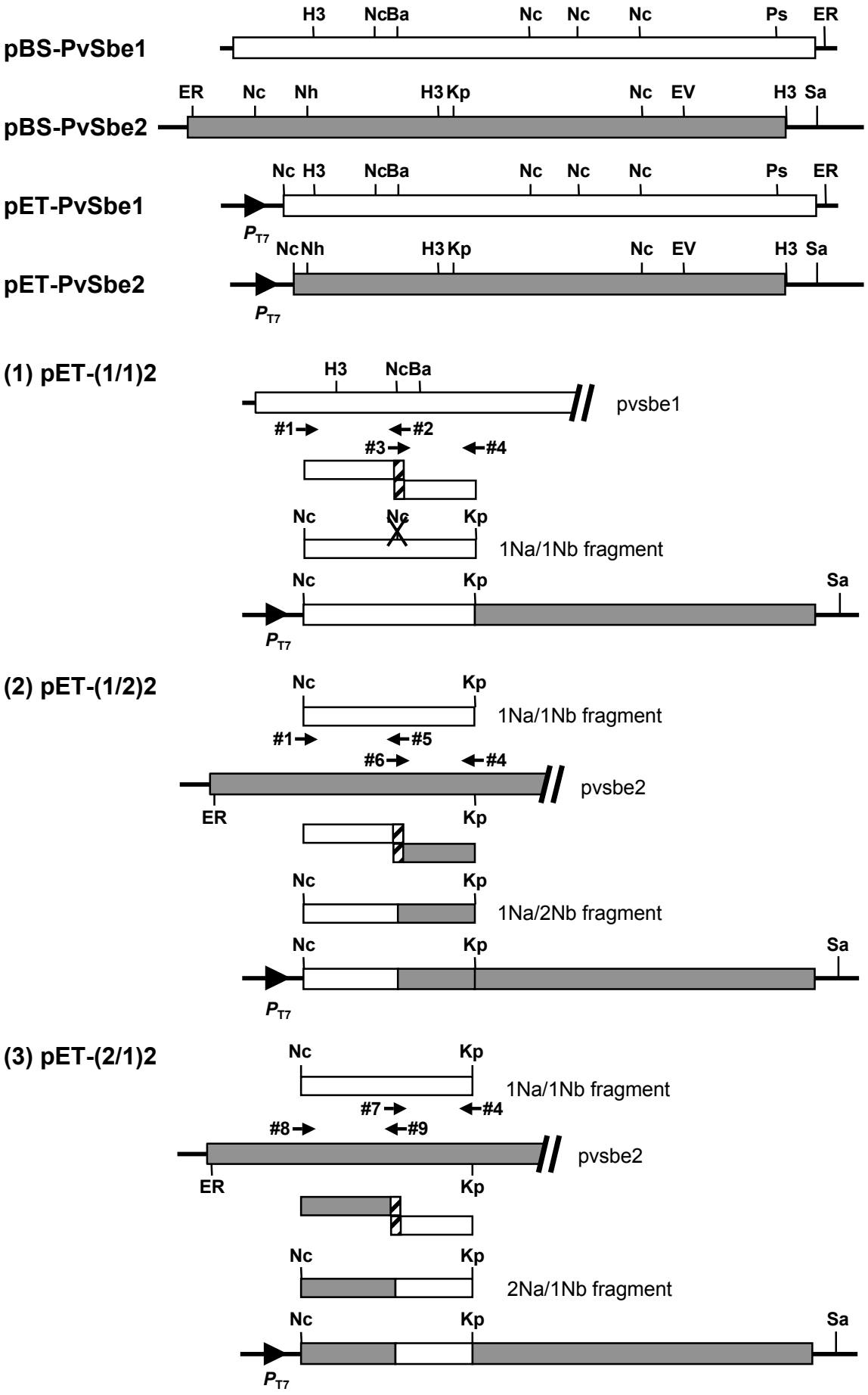

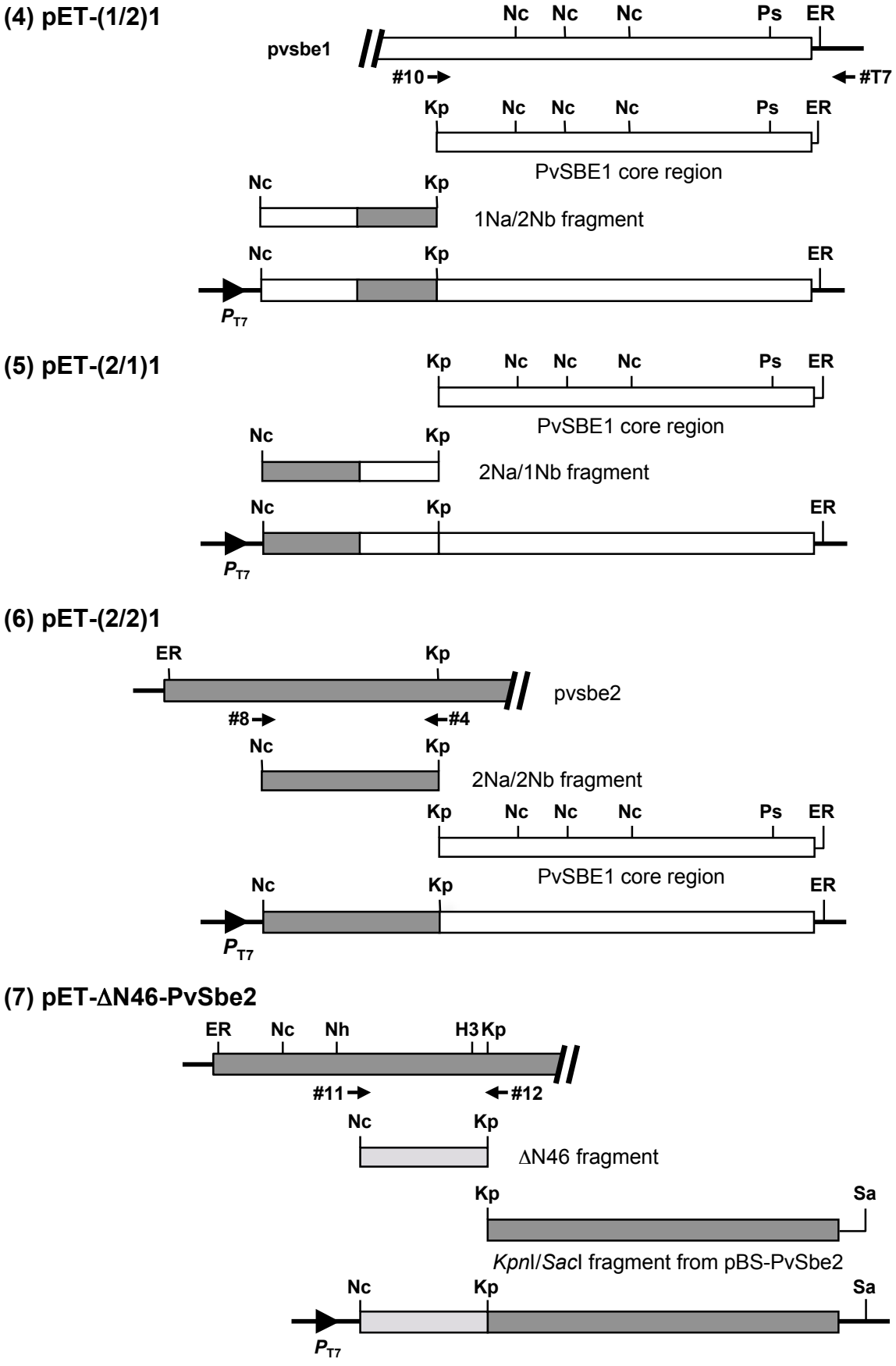

Figure S1. Construction of the expression vectors for the chimeric and N-terminal truncated enzymes

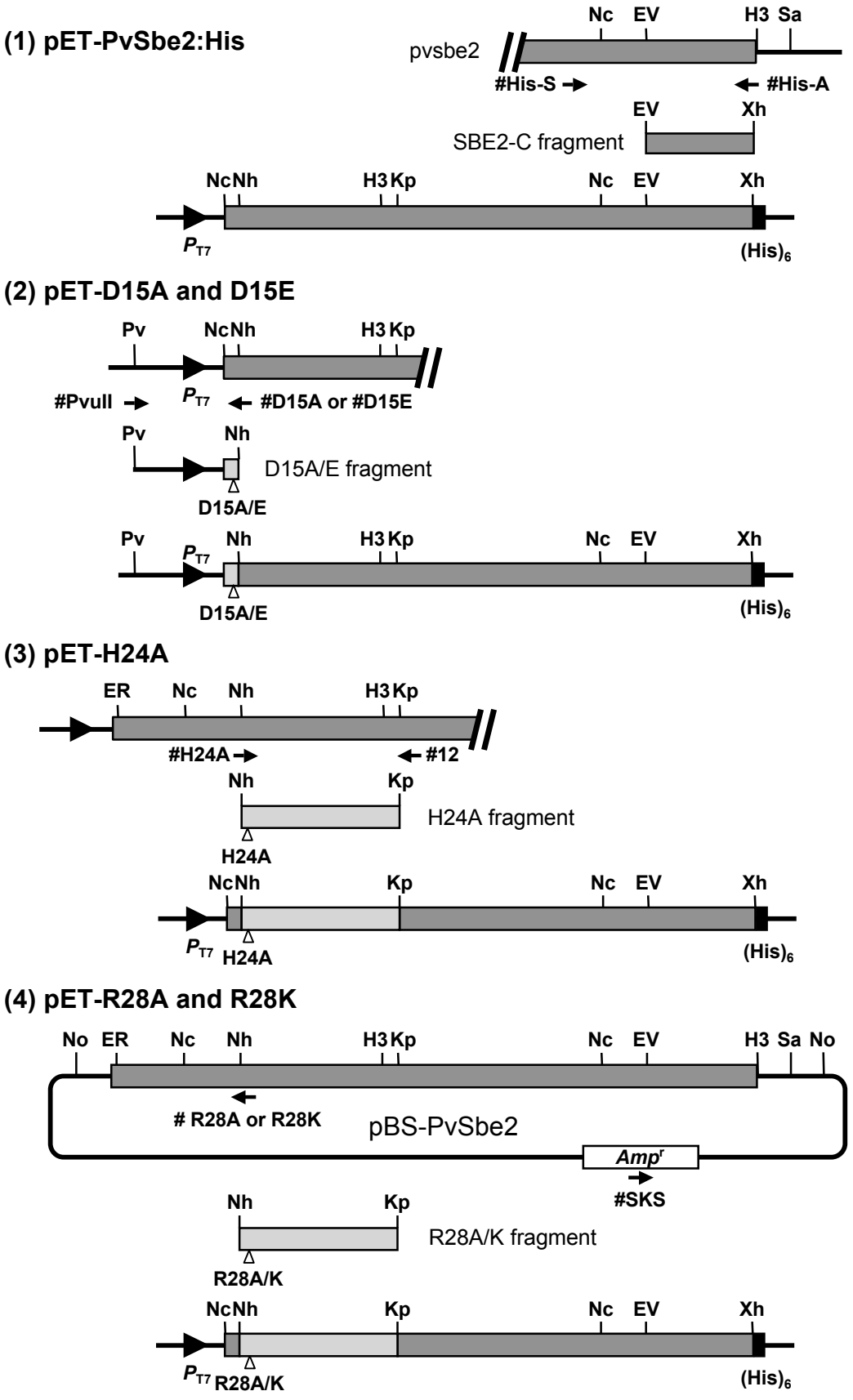

Figure S2. Construction of the expression vectors for the site-directed mutant enzymes

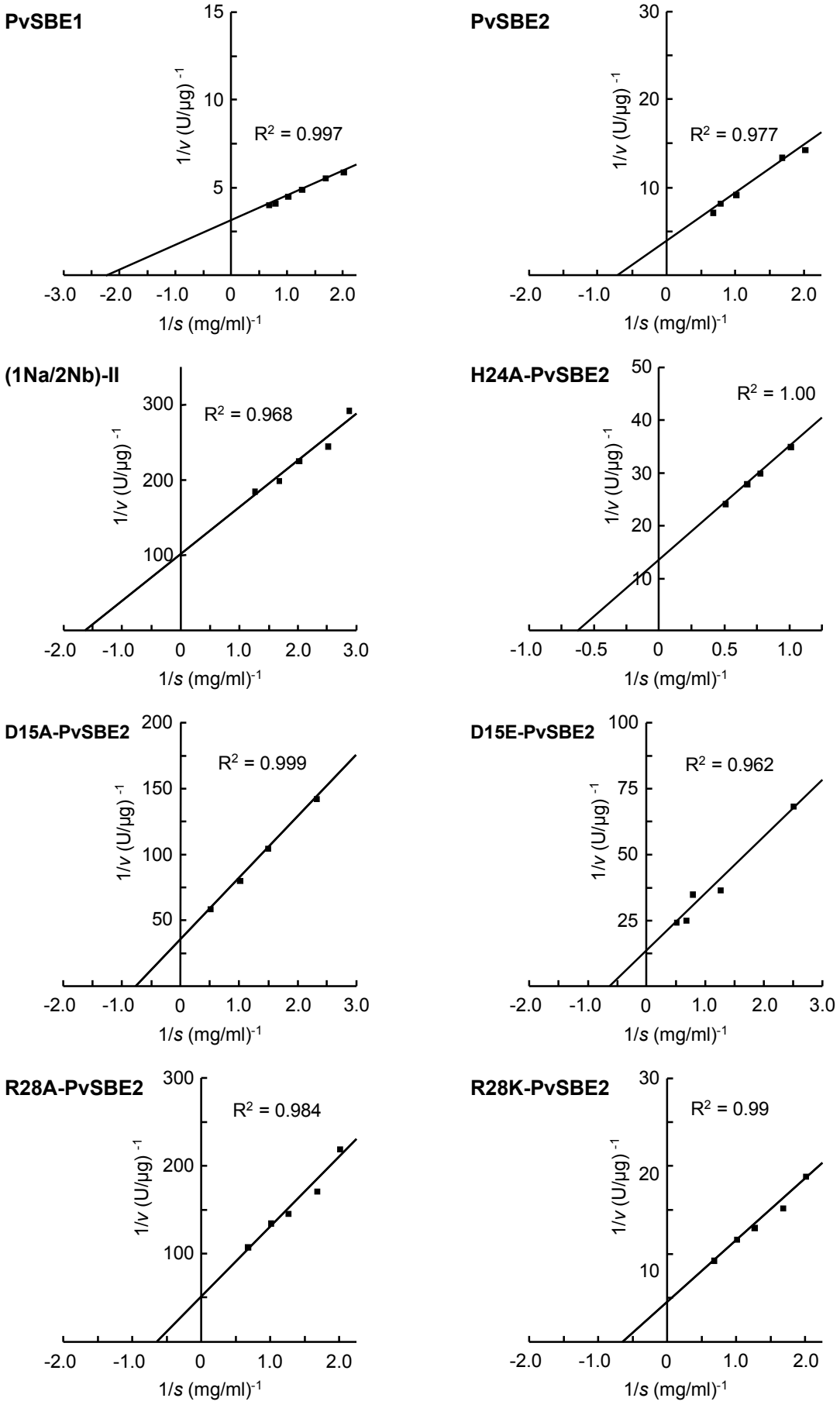

Figure S3. Double-reciprocal plots of reactions for amylose by various PvSBE enzymes.